J Pharmacol Sci **116**, 36 – 46 (2011)

Journal of Pharmacological Sciences

Full Paper

A Strong Protective Action of Guttiferone-A, a Naturally Occurring Prenylated Benzophenone, Against Iron-Induced Neuronal Cell Damage

Yanier Núñez Figueredo[1], Laura García-Pupo[1], Osmany Cuesta Rubio[2], René Delgado Hernández[1], Zeki Naal[3,4], Carlos Curti[3], and Gilberto L. Pardo Andreu[5,*]

[1]*Laboratorio de Farmacología Molecular, Centro de Investigación y Desarrollo de Medicamentos, Ave. 26, No. 1605 Boyeros y Puentes Grandes, CP 10600, Plaza de la Revolución, Ciudad Habana, Cuba*
[2]*Departamento de Farmacia and* [5]*Centro de Estudio para las Investigaciones y Evaluaciones Biológicas, Instituto de Farmacia y Alimentos, Universidad de La Habana, Ave. 23 # 21425 e/ 214 and 222, La Coronela, La Lisa, CP 13600, Ciudad Habana, Cuba*
[3]*Departamento de Física e Química, Faculdade de Ciências Farmacêuticas de Ribeirão Preto, Universidade de São Paulo, via do Café, S/N, CP 14.040-903. Ribeirão Preto, SP, Brazil*
[4]*Instituto Nacional de Ciencia e Tecnologia de Bioanalitica, UNICAMP, Campinas, SP, P.O. Box 6154, Brazil*

Received October 22, 2010; Accepted February 25, 2011

Abstract. Guttiferone-A (GA) is a natural occurring polyisoprenylated benzophenone with several reported pharmacological actions. We have assessed the protective action of GA on iron-induced neuronal cell damage by employing the PC12 cell line and primary culture of rat cortical neurons (PCRCN). A strong protection by GA, assessed by the 2,3-bis(2-methoxy-4-nitro-5-sulfophenyl)-2*H*-tetrazolium-5-carbox-anilide (XTT) assay, was revealed, with IC_{50} values <1 μM. GA also inhibited Fe^{3+}–ascorbate reduction, iron-induced oxidative degradation of 2-deoxiribose, and iron-induced lipid peroxidation in rat brain homogenate, as well as stimulated oxygen consumption by Fe^{2+} autoxidation. Absorption spectra and cyclic voltammograms of GA–Fe^{2+}/Fe^{3+} complexes suggest the formation of a transient charge transfer complex between Fe^{2+} and GA, accelerating Fe^{2+} oxidation. The more stable Fe^{3+} complex with GA would be unable to participate in Fenton-Haber Weiss-type reactions and the propagation phase of lipid peroxidation. The results show a potential of GA against neuronal diseases associated with iron-induced oxidative stress.

Keywords: guttiferone-A, iron, neuroprotection, antioxidant, iron chelation

Introduction

Oxidative stress resulting from increased iron levels has been implicated in neuronal cell death in Parkinson's disease, Alzheimer's disease, amyotrophic lateral sclerosis, multiple sclerosis, Huntington's disease, and other neurodegenerative diseases (1 – 5). Iron ions catalyze the conversion of less reactive species such as H_2O_2 and lipid peroxides into more reactive species such as hydroxyl and peroxyl/alkoxyl radicals (6). In this regard, antioxidant and iron-chelating strategies have become a focus of attention for prevention and treatment of neurodegeneration (7). Studies on the etiology of neurodegenerative diseases indicate that iron-dependent oxidative stress depletes antioxidant defense in brain (8 – 10). In fact, several iron-chelating agents exhibit neuroprotective action in animal models (11 – 13). Therefore, for effective protection against neurodegenerative diseases, the association between antioxidant and iron chelating actions may be required (14).

The interest in the antioxidant properties of polyphenols to prevent and treat neurodegenerative diseases is relatively recent, so only few compounds have been tested for these actions. For example, green tea polyphenols was reported to protect brain synaptosomes from iron-induced lipid peroxidation (15). Also, both green tea and wine polyphenols were reported to inhibit aggregation and accumulation of amyloid β (Aβ) fibrils (16) as well as to protect from Aβ neurotoxicity (17).

Guttiferone-A (GA) is a polyisoprenylated benzophe-

*Corresponding author. gilbertopardo@infomed.sld.cu
Published online in J-STAGE on April 21, 2011 (in advance)
doi: 10.1254/jphs.10273FP

none derivative (Fig. 1) firstly isolated from *S. globulifera* roots (18) and recently, by our group, from *Garcinia aristata* (Griseb.) fresh fruits (unpublished results); it is a bicyclo-[3.3.1]-nonane derivative with only one aliphatic methyl belonging to a bicyclo moiety. GA presents anti-HIV (18), cytotoxic (19), trypanocidal, antiplasmodial (20), and leishmanicidal activities (21). The presence of a planar chelating six-membered cyclic system electronically delocalized and two phenolic hydroxyl groups in the GA structure provide both antioxidant and iron-chelating potentials; these potentials, however, have been little explored. We have therefore assessed the protective action of GA on PC12 cells and primary culture of rat cortical neurons (PCRCN), as well as redox aspects in rat brain homogenate, and tried to associate this action with the GA antioxidant and iron-chelating potentials.

Materials and Methods

Reagents

All reagents were obtained from Sigma-Aldrich Corp. (St. Louis, MO, USA). Stock solutions of GA or α-tocopherol were prepared in absolute ethanol and added to the cell cultures at 1/1000 (v/v) dilution.

Isolation and identification of GA

Fresh fruits of *Garcinia aristata* (Griseb.) Borhidi were collected in the Jardín Botánico Nacional (Habana, Cuba) in July 2008 and identified by Dr. C. Victor Fuentes Fiallo. A voucher specimen (No. 700) was deposited in the Herbario del Instituto de Investigaciones Fundamentales de la Agricultura Alejandro de Humbolt. Fresh fruits (2.5 kg) were extracted with *n*-hexane (5 L × 2) for 7 days at room temperature (25°C) by using a procedure similar to that previously reported to obtain aristophenone (22). A yellow residue (7.8 g) was obtained after concentration under reduced pressure (40°C) and a portion (2 g) was purified by semi-preparative high pressure liquid chromatography (HPLC) (Phenomenex C-18 column, CH_3OH / 0.01% trifluoroacetic acid 9:1, flow rate 2.5 ml/min) in order to obtain around 0.8 g of compound 1 and 0.9 g of compound 2. These compounds were initially identified as GA and aristophenone by ^{1}H NMR and ESI-MS spectra, respectively. Compound 1 was purified by successive crystallizations from hexane solutions (purity: 99% by HPLC), and its structure was confirmed as GA by ^{1}H NMR, COSY, and HMBC spectra employing the same spectroscopic conditions previously reported (18). Briefly, the ^{1}H NMR spectrum exhibited 9 methyl groups between δ 1.24 and 1.70, an aromatic AMX spin system [δ 7.19 (d, J = 2 Hz), 6.67 (d, J = 8 Hz), 6.95 (dd, J = 2 and 8 Hz)], and five vinyl protons between δ 4.8 and 5.3. Three proton signals (δ_H 1.24 (CH_3-22) and δ_H 1.21, 1.40 (CH_2-23) showed HMBC correlations to three carbon signals at δ 68.7 (C-4), δ 51.8 (C-5), and δ 41.0 (C-6), indicating the presence of a 3-methylbut-2-enyl moiety attached to C-5 and the existence of a bicyclo-[3.3.1]-nonane derivative. All connectivities established by HMBC and COSY spectra were identical to those shown previously for GA (18). Additionally, the ESI-MS spectrum of GA showed a protonated molecule $[M+H]^+$ at m/z 603 and its fragmentation yielded ions resulting from successive elimination of the alkyl chains from the bicyclo core (18).

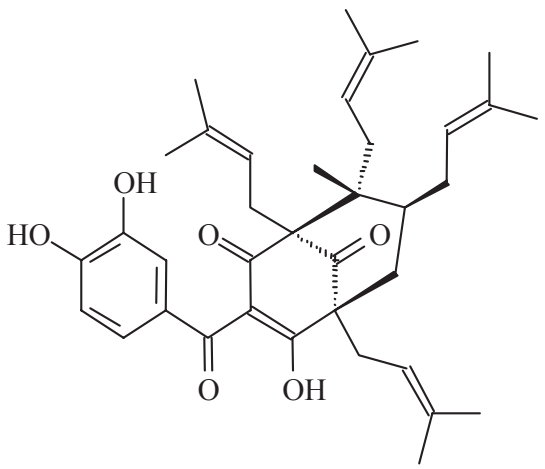

Fig. 1. Guttiferone-A (GA) structure. (1*R*,3*E*,5*S*,6*R*,7*S*)-3-[(3,4-dihydroxyphenyl)-hydroxymethylidene]-6-methyl-1,5,7-tris(3-methylbut-2-enyl)-6-(4-methylpent-3-enyl)bicyclo[3.3.1]nonane-2,4,9-trione.

Cell cultures

The pheochromocytoma (PC12) cells were a kindly gift of Dr. Beatriz Caputto from Cordoba National University, Argentina and Dr. Mari Cleide Sogayar from São Paulo University, Brazil. Cells at passage seven were routinely maintained in Dulbeccos's modified essential medium (DMEM) with L-glutamine (Sigma, St. Louis, MO, USA) and supplemented with 10% heat-inactivated equine serum (Labiofam, Havana, Cuba), 5% inactivated fetal bovine serum (Sigma), 50 U/ml penicillin, and 10 mg/ml streptomycin (Sigma) in a humidified atmosphere of 95% air / 5% CO_2, at 37°C. The growth medium was replaced every 3 days; and on day 7, cells were trypsinized (Sigma) and reseeded at a density of 1.3×10^5 cells/ml in 96-multiwell flat bottom plates (Corning Costar, Sigma) for a further 24 h incubation.

PCRCN were obtained as previously described (23), with modifications. Briefly, whole brains from 17 days embryonic Wistar rats (CENPALAB, Havana, Cuba) were kept in calcium and magnesium-free Hank's balanced salt solution (HBSS; Gibco, Paisley, UK). Cerebral

meninges-free cortices were dissected and dissociated in HBSS. Tissue pieces were incubated in trypsin (Sigma) (0.1% in HBSS) for 20 min, at 37°C, and manipulated in triturating solution using flame polished Pasteur pipettes. Cells were reconstituted in growth medium containing 85% DMEM with L-glutamine, 10% fetal bovine serum, 50 U/ml penicillin, and 10 mg/ml streptomycin. Viable cells, demonstrated by trypan blue exclusion, were plated on poly-L-lysine (Sigma) (0.01% in distilled water)-coated 96-multiwell flat bottom plates (Corning Costar, Sigma) at a density of 5×10^5 cells/ml. The cell culture was incubated in a humidified atmosphere of 95% air / 5% CO_2, at 37°C, and used after 24 h. The protocol of animal experiments was approved by the Animal Experimentation Ethics Committee of Havana University.

Assessment of GA cytotoxicity

PC12 cells (1.3×10^5 cells/ml) or PCRCN (5×10^5 cells/ml), seeded in 96-multiwell flat bottom plates, were incubated with different GA concentrations (0.001 – 50 μM) or absolute ethanol (0.001% in growth medium) as vehicle control, for 48 h. After incubation, cell viability was measured using the 2,3-bis(2-methoxy-4-nitro-5-sulfophenyl)-2*H*-tetrazolium-5-carbox-anilide (XTT) reduction assay, according to the manufacturer's protocol. Briefly, 0.05 ml XTT labelling mixture was added per well and after 4 h incubation in 5% CO_2, at 37°C, absorbance at 450 nm was determined in a microplate reader.

Induction of cell oxidative damage and treatment with GA

The neuroprotective action of GA was tested on PC12 cells and PCRCN (0.001 – 50 μM) by means of two experimental approaches: i) pre-incubation of cells for 24 h with GA or α-tocopherol (1 mM) before inducing oxidative damage with $FeSO_4$ (5 mM) and ascorbic acid (2 mM), and ii) co-incubation for 24 h with GA or α-tocopherol (1 mM), $FeSO_4$ (5 mM), and ascorbic acid (2 mM). After 24 h, the cell supernatant was removed and cell viability was measured by the XTT assay (see above).

Determination of Fe^{2+} concentration

The concentration of Fe^{2+} was determined in 10 mM phosphate buffer pH 6.5 (2 ml) by the formation of a red complex with 1,10-phenanthroline (5 mM), as previously described (24).

Oxygen consumption monitoring

Oxygen consumption associated to ferrous ion oxidation was polarographically monitored with a Clark-type electrode (Hansatech Instruments, Pentney King's Lynn, UK) in a 1.3-ml glass chamber equipped with a magnetic stirrer, at 30°C. The rate of oxygen consumption (ROC) was expressed as nmol O_2/ml per min.

Lipid peroxidation assay

Lipid peroxidation was assessed by malondialdehyde (MDA) production in rat's brain homogenate, as previously described (25), with few modifications. Briefly, rats were sacrificed by diethyl ether intoxication and whole brains were dissected out. Then, brains were washed in saline solution, weighed, minced quickly, and homogenized in 4 ml of cold phosphate buffer (50 mM, pH 6.5) per gram of wet weight, using a Potter Elvehjem-type tissue homogenizer. The homogenate was centrifuged at 2000 × *g* for 10 min at 4°C and diluted supernatant (1:3 in cold phosphate buffer) was used for MDA determination. Homogenate oxidation mixtures in the presence of $FeCl_3$ and ascorbic acid (100 mM final concentrations) were heated at 37°C for 60 min and 0.4 ml was included in the final reaction mixture with 0.25 ml trichloroacetic acid (100%) and 0.05 ml thiobarbituric acid (12 M). This final mixture were strongly stirred and incubated further for 30 min in 100°C heated water. Finally, the cooled mixture (25°C) was centrifuged for 15 min at 1000 × *g* and absorbance at 532 nm was determined in the supernatant. MDA concentration was calculated from $\varepsilon = 1.56 \times 10^5\ M^{-1} \cdot cm^{-1}$ (26).

2-Deoxyribose oxidation assay

The formation of hydroxyl ($^{\bullet}OH$) radicals was assessed through 2-deoxyribose oxidative degradation; it produces MDA, which condensates with thiobarbituric acid, forming a coloured adduct (27). Typical reactions were started by addition of ascorbate (0.1 mM final concentration) to a solution containing 10 mM phosphate buffer (pH 7.2), 2.8 mM 2-deoxyribose, 0.1 mM ethylendiamine tetracetic acids (EDTA), 25 μM $FeCl_3$, and 2.8 mM H_2O_2, in the absence or presence of GA (0.01 – 100 μM). Reactions were carried out for 1 h at 37°C in a shaking bath to ensure continuous flow of O_2 into the tubes and terminated by the addition of 1 ml of 2.8% (w/v) trichloacetic acid followed by 1 ml 1% thiobarbituric acid solution in 50 mM NaOH. After heating at 80°C for 20 min, absorbance at 532 nm was determined.

Determination of Fe^{2+} and Fe^{3+} complexes with GA

Fe^{2+} ($FeCl_2$, 10 – 200 μM final concentration) and Fe^{3+} ($FeCl_3$, 12.5 – 100 μM final concentration) were added to 2 ml 10 mM phosphate buffer (pH 6.5) containing 2 mM citrate and 50 μM GA (2 ml final volume). An immediate wavelength scan from 200 – 400 nm was performed in a Hitachi 2001 spectrophotometer (Hitachi, Tokyo), at 28°C. This allowed the observation of changes in the

characteristic peak of GA at a wavelength near 270 nm due to formation of Fe^{2+}/Fe^{3+}–GA complexes. As in the electrochemical experiments, aliquots of the acidic aqueous fresh solution of $FeCl_3$ or $FeCl_2$ were added to give the solutions at the desired concentrations.

Electrochemical assays

Electrochemical assays were carried out with a BAS CV-27 potentiostat (Bioanalytical System, Inc., West Lafayette, IN, USA) by employing conventional electrochemical cells with three electrodes; the data were recorded on an Omnigraphic 100 recorder (Texas Instruments, Houston, TX, USA). A glassy carbon electrode with 0.0314 cm^2 geometric area, polished with 1 μm alumina–water suspension and rinsed thoroughly with water and acetone, was used as working electrode. A platinum wire was used as the counter electrode and all potentials are referenced to a sodium saturated silver/silver chloride electrode [Ag/AgCl/KCl(sat)] without regard for the liquid junction potential. The cyclic voltammetric studies were carried out at 100 mV/s sweep rate in 5 ml of 0.1 M phosphate buffer solution (pH 7), where aliquots of 100 mM dimethyl sulfoxide (DMSO) solution of GA were added. Since the cyclic voltammograms were recorded at a window potential including negative ranges, oxygen-free solution was obtained by bubbling argon through it. When the potential was scanned, the inert gas was kept in the solution to ensure that any oxidation reaction was not begun by oxygen. For the electrochemical process of GA in the presence of Fe^{3+}, aliquots of a fresh acidic aqueous solution of $FeCl_3$ were added to give final concentrations of 100, 250, and 450 μM. For the electrochemical process of GA in presence of Fe^{2+}, aliquots of GA in DMSO (210 μM final concentration) were added to 2 mM $FeCl_2$ solution in 0.1 M acetate/acetic acid buffer (pH 5). The solutions were stirred for 30 s and allowed to rest for 30 s for equilibration.

Statistical analyses

All the data are expressed as a mean ± S.D. ANOVA with the Bonferroni post hoc test or *t*-test were used for statistical comparison of the experimental group where appropriate, with statistical significance set at $P < 0.05$. SPSS10 software (SPSS, Chicago, IL, USA) was used for data analyses.

Results

Effects of GA on cell viability

The effects of GA on PC12 cells and PCRCN viability were assessed after 48 h incubation through the XTT reduction assay. Figure 2 shows that in the concentration range used for the protection assay (up to 50 μM), GA was not toxic to either PC12 cells or PCRCN.

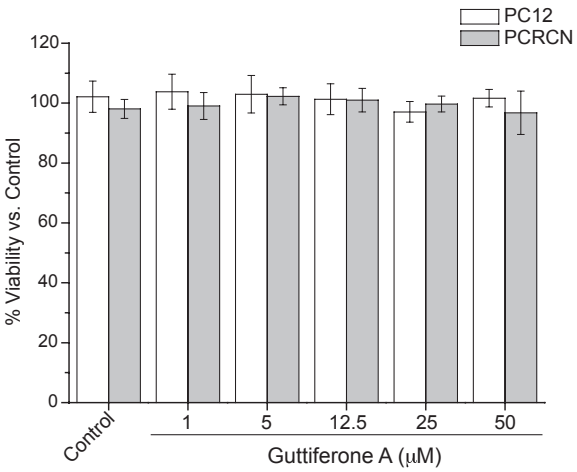

Fig. 2. Effects of GA on PC12 cells and primary culture of rat cortical neurons (PCRCN) viabilities. The assay conditions are described in Materials and Methods. Values are each the mean ± S.D. of three different experiments.

Protective effects of GA on Fe^{2+} toxicity

Pre-incubation or co-incubation with GA significantly increased the viability of iron-overloaded cells. This protective effect started at 0.01 and 0.05 μM for PC12 cells and PCRCN, respectively (Fig. 3: A and B). Pre-incubations of both PC12 cells and PCRCN with GA were more effective than co-incubations (Fig. 3: A and B), as attested by the lower IC_{50} values.

Fe^{2+}–citrate autoxidation / O_2 consumption induced by GA

GA decreased Fe^{2+} levels in a concentration-dependent manner after 5 min incubation with 1 mM citrate (Fig. 4A). The addition of ascorbic acid (2 mM final concentration) to the GA–iron mixture partly restored ferrous ions levels (Fig. 4A). GA also increased the ROC, in apparent association with its stimulatory effect on oxidation of Fe^{2+} to Fe^{3+} (Fig. 4: B and C). In Fig. 4B, line a represents the time-course of oxygen consumption associated with the oxidation of 50 μM Fe^{2+} to Fe^{3+} in the absence of GA (ROC = 91.39 ± 4.32 nmol O_2/ml per min). Increasing concentrations of GA enhanced ROC associated to ferrous ions oxidation: 115.3 ± 5.16, 184.0 ± 3.94, 203.8 ± 4.48, and 234.68 ± 5.25 nmol O_2/ml per min when Fe^{2+} was incubated with 25 (line b), 50 (line c), 100 (line d), and 200 (line e) μM GA, respectively. We have used 1,10-phenantroline to measure the levels of Fe^{2+} formation from Fe^{3+} solution (50 μM) in presence of 2 mM ascorbate and GA, as well as the rate

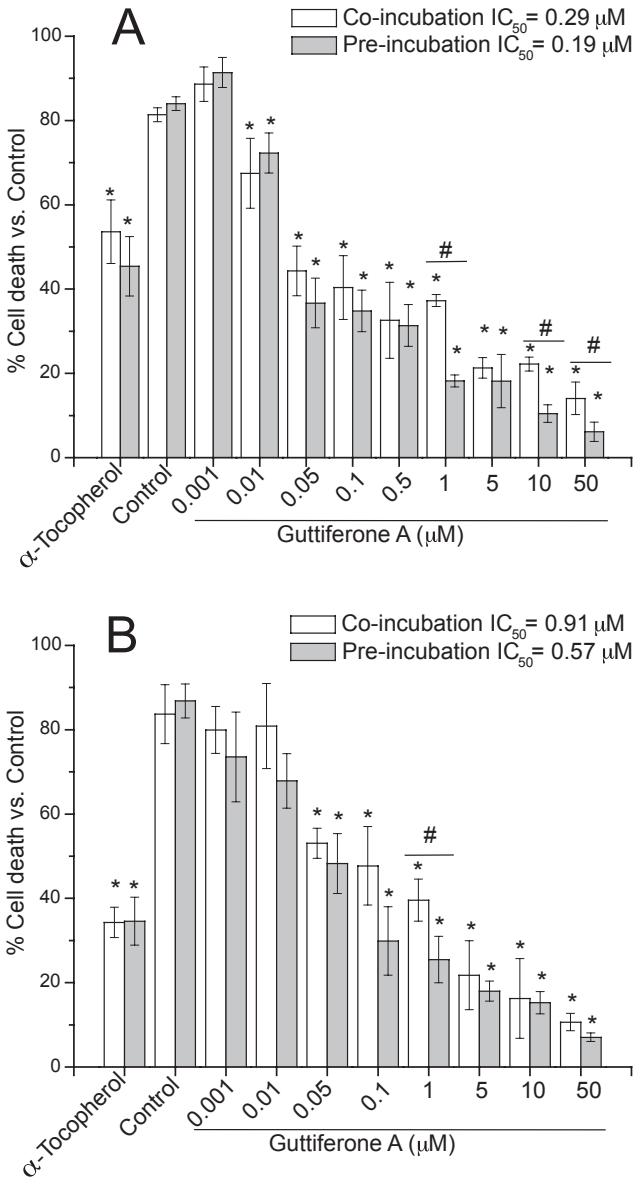

Fig. 3. GA protection against iron-induced neuronal cell damage. PC12 cells (A) and PCRCN (B) viability, assessed by the XTT assay. Cells were seeded at a density of 1.3×10^5 and 5×10^5 cells/ml, respectively, in 96-multiwell flat bottom plates. GA (0 – 50 μM) or α-tocopherol (1 mM) were pre-incubated for 24 h before addition of 5 mM $FeSO_4$ and 2 mM ascorbate (gray columns) or were co-incubated with these agents for 24 h (white columns). The supernatant was removed, cells were incubated with 25 μg XTT for 4 h and absorbance at 450 nm was determined. Control cells (without GA), contained absolute ethanol (0.001%) plus the iron-ascorbate mixture. The results are expressed as percentage of cell death in relation to the control. Values are each the mean ± S.D. of three different experiments. $^*P < 0.05$ vs. control cells; $^{\#}P < 0.05$, co-incubation vs. pre-incubation.

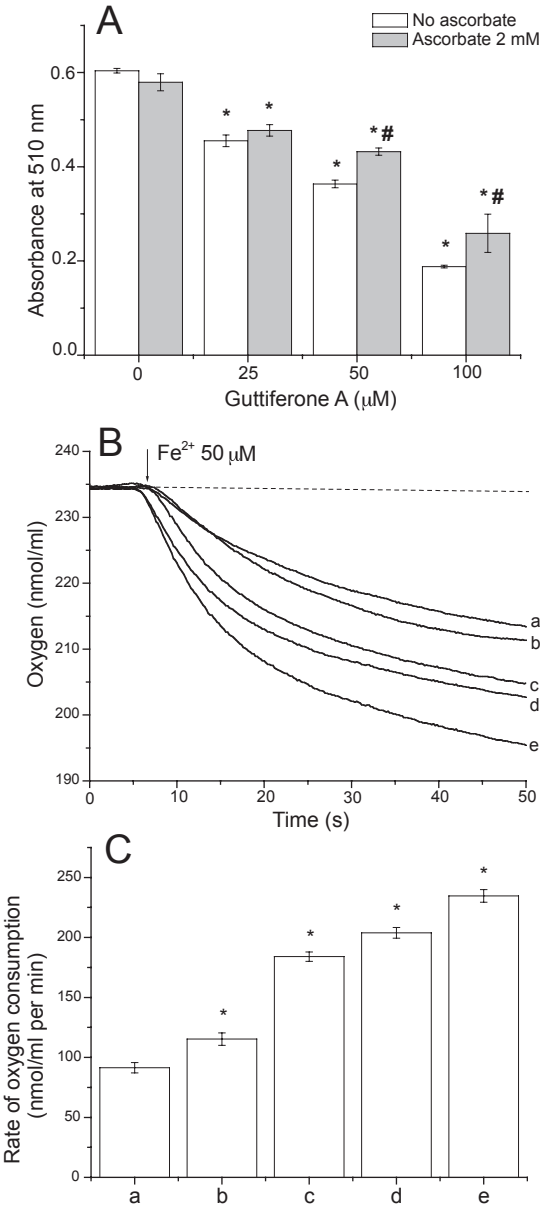

Fig. 4. GA promotes a diminution in Fe^{2+} concentrations. A) Stimulation of Fe^{2+} autoxidation by GA. The reaction medium contained GA (0 – 100 μM), 2 mM citrate, and 10 mM phosphate buffer, pH 7.2. An excess of 1,10 phenantroline (5 mM) was added immediately after 50 μM Fe^{2+} addition and absorbance was determined at 510 nm (white columns). Ascorbate (2 mM) was added 1 min after Fe^{2+} addition and absorbance was determined again at 510 nm (gray columns). Experiments were conducted at 30°C with agitation and were started by the addition of 50 μM $FeCl_2$. Values are each the mean ± S.D. of three different experiments. $^*P < 0.05$ vs. experiment without GA. $^{\#}P < 0.05$ vs. the same experiments without ascorbate. B) Effects of GA on O_2 consumption induced by Fe^{2+} autoxidation. Experimental conditions were the same as in panel A: a) No GA; b) 25, c) 50, d) 100, and e) 200 μM GA. Dashed line indicates O_2 consumption in reaction medium without Fe^{2+} addition. Traces are representative of three assays. C) Rate of oxygen consumption after 20-s incubation. Legends are the same as in panel B. Values are each the mean ± S.D. of three different experiments. $^*P < 0.05$ vs. the experiment without GA (line a).

of O_2 consumption due to autoxidation of Fe^{2+} originated from Fe^{3+}–ascorbate reduction. Figure 5A shows that GA inhibits the reduction of ferric ions elicited by ascorbate,

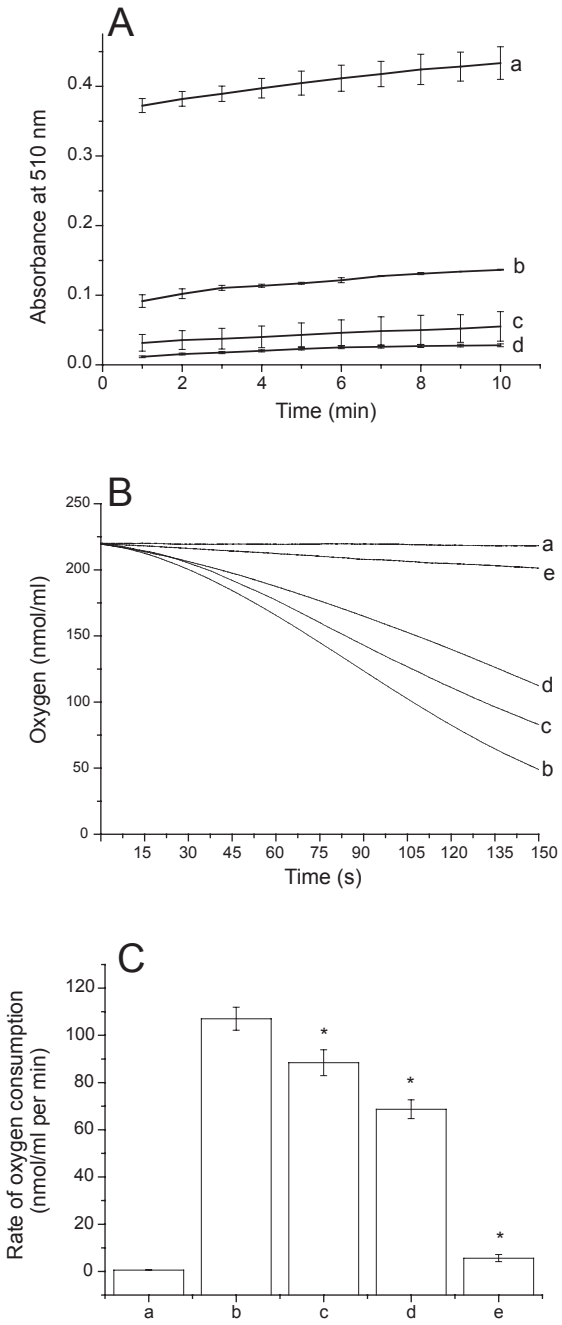

Fig. 5. GA inhibits Fe^{3+} reduction induced by ascorbate. A) Inhibition by GA of ascorbate-induced Fe^{3+} reduction, after 10-min incubation in a medium consisting of GA (0 – 100 μM), 2 mM citrate, 50 μM $FeCl_3$, and 5 mM 1,10-phenanthroline in 10 mM phosphate buffer, pH 7.2, at 28°C. Reaction was initiated with 2 mM ascorbate and absorbance at 510 nm was determined: a) No GA; b) 25, c) 50, and d) 100 μM GA. Values are each the mean ± S.D. of three different experiments. B) Effects of GA on O_2 consumption by Fe^{2+} (formed by Fe^{3+}–ascorbate reduction) autoxidation, under the same experimental condition described in panel A. Reaction was initiated with 2 mM ascorbate (except in line a): a) 100 μM GA, no ascorbate addition; b) no GA; c) 25, d) 50, and e) 100 μM GA. Traces are representative of three assays. C) Rate of oxygen consumption after 90-s incubation, as described in panel B. Values are each the mean ± S.D. of three different experiments. *$P < 0.05$ vs. experiment without GA (line b).

in a concentration-dependent manner, reaching near full inhibition at 100 μM. These results suggest a composition of 2:1 for the GA–Fe^{3+} complex at pH 7.2 and low iron concentrations. Figure 5B confirms these results. Line a shows an almost null oxygen consumption in 50 μM ferric solution with 100 μM GA (without ascorbate), indicating no reduction process in ferric ions (ROC = 0.58 ± 0.11 nmol O_2/ml per min). Line b shows oxygen consumption due to Fe^{2+} (formed by Fe^{3+}–ascorbate reduction) autoxidation (ROC = 107.0 ± 4.87). Lines c, d, and e show inhibitory effects of 25, 50, and 100 μM GA, respectively, on Fe^{2+} formation from Fe^{3+}–ascorbate reduction. ROC values were 88.39 ± 5.45, 68.72 ± 3.97, and 5.63 ± 1.48 nmol O_2/ml per min, respectively.

GA effects on iron-induced lipid peroxidation

Rat brain phospholipids undergo a rapid non-enzymatic peroxidation, yielding MDA, when exposed to ferric chloride and ascorbic acid. GA inhibited MDA formation in rat brain homogenate incubated with Fe^{3+}–ascorbate mixture (Fig. 6).

GA effects on 2-deoxyribose oxidative degradation

Competition studies were performed to assess the effectiveness of GA, compared to the classical $^{\bullet}OH$ scavenger DMSO (20 mM), to protect 2-deoxyribose (2.8 mM) from iron-mediated oxidative damage (Fig. 7). Protection by GA at the micromolar concentration range was far more effective than protection by DMSO at the

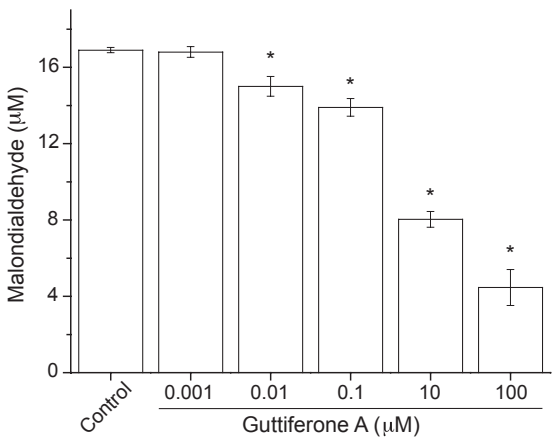

Fig. 6. Inhibition by GA of iron-induced lipid peroxidation (malondialdehyde) in rat brain homogenate. Rat brain homogenate was incubated in the presence of $FeCl_3$ and ascorbate (both at 100 mM final concentration), without (control) or with GA (0.001 – 100 μM). An aliquot was mixed with 100% TCA and 12 M thiobarbituric acid for developing the coloured product. The control contains only absolute ethanol (0.001%), which is the solvent concentration in the GA samples. Values are represent the mean ± S.D. (n = 6). *$P < 0.05$ vs. control.

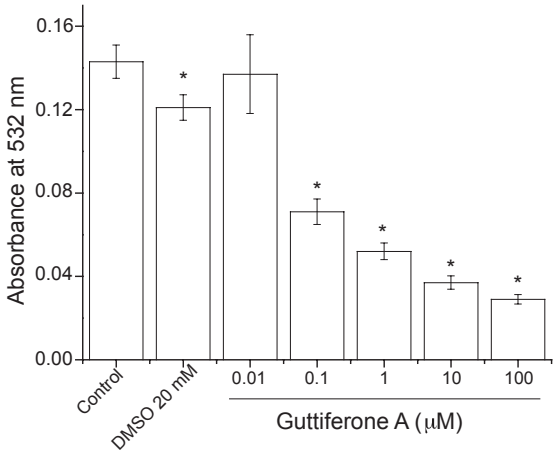

Fig. 7. Effects of GA and the ·OH scavenger DMSO on oxidative damage of 2-deoxyribose (2.8 mM) induced by $FeCl_3$–EDTA plus ascorbate. Solutions were incubated for 60 min at 37°C in a medium consisting of 10 mM phosphate buffer (pH 7.2), 2.8 mM 2-deoxyribose, 0.1 mM EDTA, 2.8 mM H_2O_2, and 25 μM $FeCl_3$. Reactions were initiated with 0.1 mM ascorbate (final concentration). Controls contain only absolute ethanol (0.001%), which is the solvent concentration in the GA samples. Values represent the mean ± S.D. (n = 3). *$P < 0.05$ vs. control.

millimolar concentration range.

Spectrophotometric and electrochemical evidences for GA-iron interaction

Since oxidation of Fe^{2+} via direct electron abstraction by GA seems unlikely under aerobic conditions, one hypothesis is that GA forms a charge transfer complex with ferrous iron facilitating its oxidation by oxygen. This transition complex with Fe^{2+} could deliver its electrons more readily than the Fe^{2+}–citrate complex and then form a more stable complex with Fe^{3+}. To test this hypothesis, absorption spectra of samples containing 70 μM GA with increasing concentrations of Fe^{2+} (12.5 – 100 μM $FeCl_2$) or Fe^{3+} (10 – 200 μM $FeCl_3 \cdot 6H_2O$) were done in 10 mM phosphate buffer (pH 7.0) containing 2 mM citrate. Figure 8 shows a typical spectrum of GA with maximum absorption at 273 nm (line a). Addition of either Fe^{2+} or Fe^{3+} induced a concentration-dependent increase in the maximum absorption of GA (Fig. 8A, lines b – h and Fig. 8B, lines b – i). The occurrence of a new family of spectra originated from GA spectrum was confirmed by the presence of an isosbestic point at a wavelength near 340 nm, which could be ascribed to the GA–Fe^{3+}-complex equilibrium.

Figure 9A shows a series of consecutive cyclic voltammograms for a glassy carbon electrode in contact with the 0.25 mM solution of GA in 10 mM phosphate buffer (pH 7.2). The first scan to positive potentials showed two

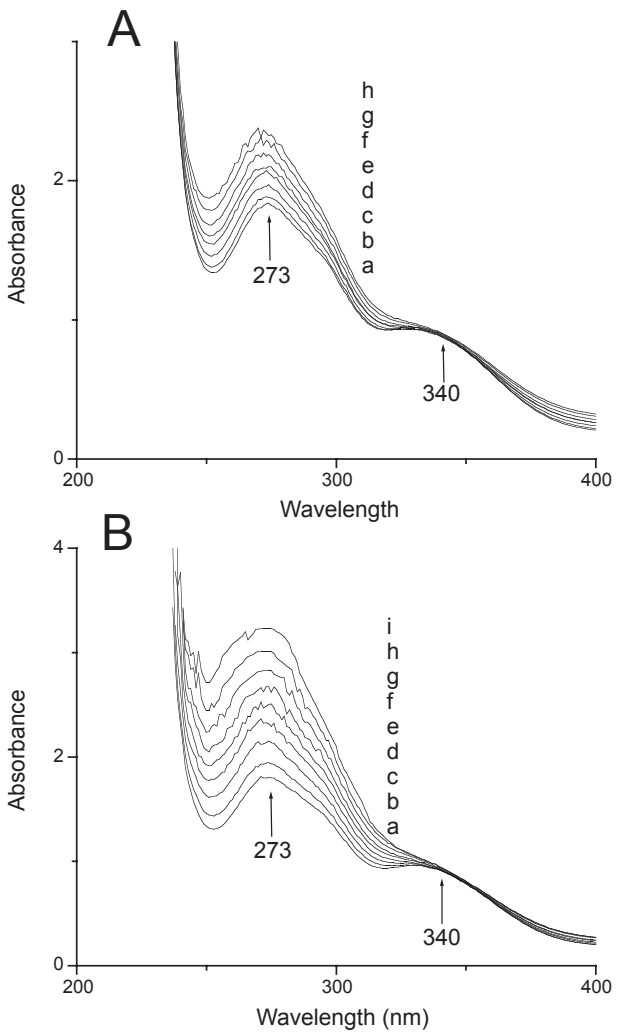

Fig. 8. Spectrophotometric evidences of GA–iron ions interaction. Effects of $FeCl_2$ (Fe^{2+} ions) (A) and $FeCl_3$ (Fe^{3+} ions) (B) on GA UV–VIS spectrum (200 – 400 nm), in a incubation medium consisting of 10 mM phosphate buffer (pH 7.2), 2 mM citrate, and 70 μM GA, at 28°C. Panel A: a) no $FeCl_2$ addition; b) 10, c) 30, d) 50, e) 70, f) 100, g) 130, and h) 160 μM $FeCl_2$. Panel B: a) no $FeCl_3$ addition; b) 12.5, c) 25, d) 37.5, e) 50, f) 62.5, g) 75, h) 87.5, and i) 100 μM $FeCl_3$. Scan speed was 2 nm/s. Typical tracings of three independent experiments are shown.

irreversible oxidation peaks at +0.250 and +0.40 V (left arrow), whose amplitude decreased upon second scanning and that we ascribe to a catechol oxidation process. In the second sweep, there was no peak, which we ascribe to a surface-localized process, analogous to another catechol derivative studied earlier (28). Figure 9, B – D, shows another series of cyclic voltammograms after addition of aliquots of Fe^{3+} solutions to give concentrations of 100, 250, and 450 μM, respectively. It should be noted that there was a significant increase in the anodic current at +0.4 V when the concentration of Fe^{3+} increases. There

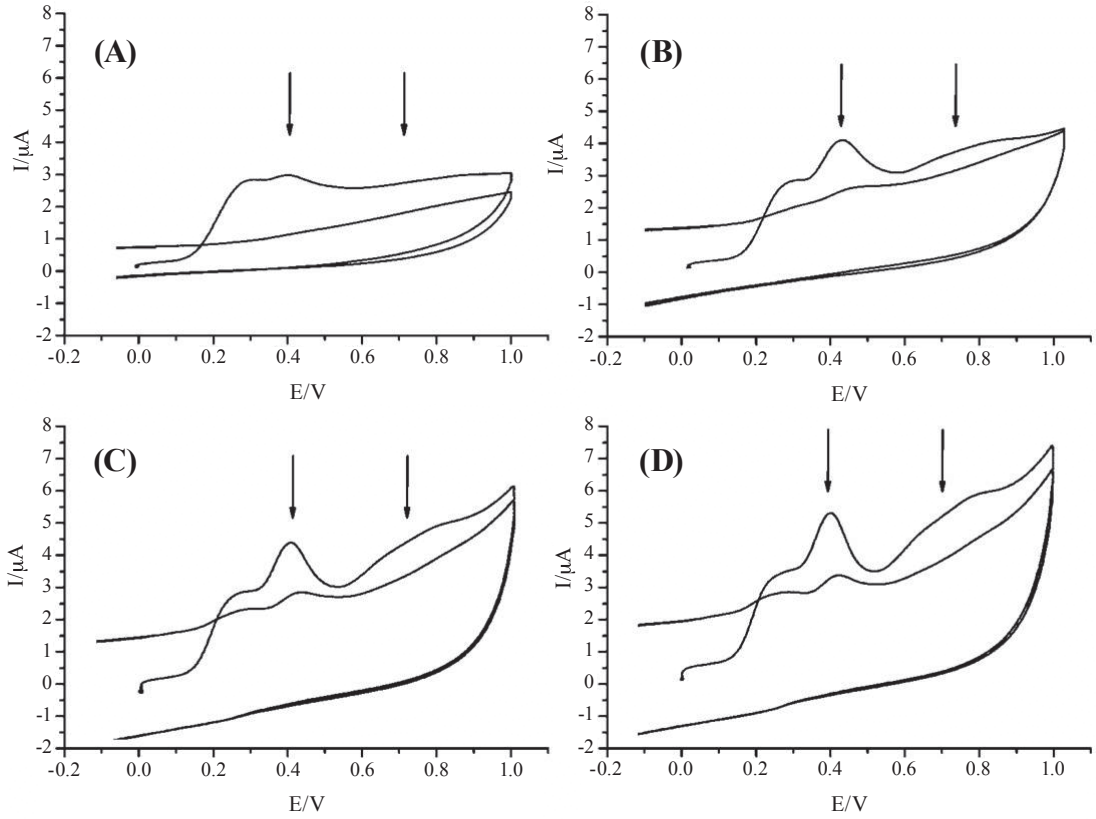

Fig. 9. Cyclic voltammograms of 0.25 mM GA in the presence of 0 (A), 100 (B), 250 (C), and 450 (D) μM $FeCl_3$, in an aqueous solution plus 10 mM phosphate buffer (pH 7.2). The scan rate was 100 mV/s, using a glassy carbon electrode (area 0.0314 cm^2) as the working electrode. Typical tracings of three independent experiments are shown.

is also an additional broad peak, with a potential value around +0.70 V (right arrow), that could be ascribed to the oxidation of the catechol group coordinated to Fe^{3+}. These results and the evidence that a catechol redox process may occur in the presence of Fe^{3+} (second scan) suggest that GA becomes coordinated to Fe^{3+}.

Figure 10 shows cyclic voltammograms of a solution of Fe^{2+} in acetate buffer (pH 5), in order to avoid hydrolysis, in absence or presence of GA. Anodic peak in curve a at +0.45 V could be ascribed to oxidation of Fe^{2+} to Fe^{3+}, and the consecutive reduction at −0.055V. In the presence of 210 μM GA, the oxidation and reduction peak decreased significantly when the scan rate was 20 mV/s (peak b). This difference was smaller when the scan rate was 100 mV/s (data not shown), confirming the interaction between Fe^{3+} and GA.

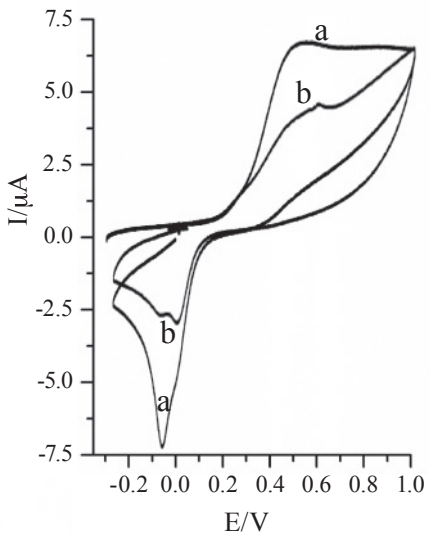

Fig. 10. Cyclic voltammograms of 2 mM $FeCl_2$ in the presence of 0 (a) and 210 (b) μM GA in 0.1 M acetate/acetic acid buffer (pH 5). The scan rate was 20 mV/s, using a glassy carbon electrode (area 0.0314 cm^2) as working electrode. Typical tracings of three independent experiments are shown.

Discussion

PC12 is a cell line derived from rat pheochromocytoma which displays features of neuronal cells. Together with PCRCN, this cell line has been widely used as model for

the investigation of neurodegeneration/neuroprotection and for testing potential neuroprotective compounds (28 – 34). A previous study demonstrated that iron and ascorbic acid synergistically induce apoptosis in PC12 cells with the involvement of lipid peroxidation and depletion of reduced glutathione (35). Here we have assessed the protective action of GA on PC12 cells and PCRCN incubated with an iron/ascorbate mixture and a strong protection against iron-induced oxidative cell damage was revealed.

The ability of GA to decrease ferrous ions concentration in association with increase in the rate of oxygen consumption suggests that it removes Fe^{2+} from the citrate complex, oxidizing it to a ferric form in a process that requires O_2 as an electron acceptor. Therefore, GA decreases the amount of Fe^{2+} involved in the formation of $^{\bullet}OH$ radical through Fenton-Haber Weiss-type reactions. The lack of major spectral differences between the two GA complexes (with Fe^{2+} or Fe^{3+}) may not be only due to oxidation of Fe^{2+} to Fe^{3+}, but also due to reduction of Fe^{3+} to Fe^{2+} by GA, which could reload biological systems with Fe^{2+}. The GA–Fe^{3+} complex could allow the oxidation of biologically relevant reducing agents like ascorbate, with consequent formation of Fe^{2+}. GA inhibited the ascorbate-mediated reduction of Fe^{3+} to Fe^{2+}, excluding a direct reduction of Fe^{3+} by GA as an explanation for the absence of major spectral differences between GA–Fe^{2+} and GA–Fe^{3+} complexes. The hypothesis that GA strongly interacts with iron is also demonstrated through the spectrophotometric and electrochemical techniques.

These results show for the first time that GA protects neuronal cells from iron-induced death, probably through its ability to interact with the metal, rendering it inactive for participation in catalytic reactive oxygen species formation through Fenton–Haber–Weiss reactions. They suggest, in addition, the formation of a transient charge transfer complex between Fe^{2+} and GA, accelerating Fe^{2+} oxidation and formation of a more stable Fe^{3+}–GA complex unable to participate in Fenton–Haber–Weiss reactions and the propagation phase of lipid peroxidation. Indeed, a biologically relevant reducing agent like ascorbate was unable to reduce ferric iron in the presence of GA. In this regard, GA at micromolar concentrations was more effective than DMSO at millimolar concentrations in protecting 2-deoxyribose from iron-mediated oxidation. This suggests that GA, unlike typical $^{\bullet}OH$ scavengers, does not interfere with the reaction between 2-deoxyribose and $^{\bullet}OH$ radicals, supporting the notion that it acts by preventing $^{\bullet}OH$ formation from Fe^{3+}–EDTA plus ascorbate rather than by trapping $^{\bullet}OH$ radicals.

Two important aspects of the present results should be considered: i) a significant reversal of the iron-induced cytotoxicity was observed for GA concentrations below 1 μM and ii) pre-incubation of cells with GA was more effective than co-incubation. Therefore, GA confers cell protection by stimulating other cellular antioxidant/cytoprotective mechanisms in addition to its chelating/direct antioxidant properties. We believe the lipophilic character of GA could allow it to insert into cellular membrane and to prevent lipid peroxidation in situ. Indeed, the observed inhibition of lipid peroxidation by GA supports this hypothesis, particularly in PCRCN where the high levels of unsaturated fatty acids may increase their sensibility to oxidative stress. On the other hand, the high efficacy of GA to prevent iron-induced cell damage could be explained by the formation of a redox active GA–Fe^{3+} complex. It may mimic superoxide dismutase activity maintaning the Fe-chelate within a continuous Fe^{3+}–Fe^{2+}–Fe^{3+} conversion, avoiding significant accumulation of Fe^{2+} or superoxide. In this regard, we recently demonstrated that the 2:1 mangiferin–Fe^{3+} complex was more effective than mangiferin alone, a catechol containing polyphenol, in scavenging reactive oxygen species and in protecting hepatocytes and isolated mitochondria from oxidative stress (36 – 38).

It is well established that chelating agents by which oxygen serves as iron ligand promote oxidation of Fe^{2+}, stabilizing Fe^{3+}, thus decreasing its reducting potential (39). At physiological pH, catechols readily form thermodynamically stable bis complexes with ferric iron as bidentate ligands, favoured by low concentrations. The presence of a catechol moiety in the GA structure suggests such mechanism of iron interaction, which could explain the protection afforded against iron-induced neuronal cell damage. In this regard, we also previously demonstrated that mangiferin stimulates ferrous iron oxidation and prevents ferric iron reduction as at least part of its antioxidant mechanism (40 – 43).

It should be noted that at low micromolar concentrations GA was able to produce more than 50% protection against damage induced by millimolar concentrations of iron. Since in vivo the levels of free or loosely bound iron are hardly higher than 1 μM, even under iron overload (44), less than 2 μM GA (considering a 2:1 ratio for the GA–iron complex) would afford protection against iron-mediated cell damage. This represents around 2 μg/ml of GA, a concentration feasible to be reached in vivo. Therefore, GA may cross the blood–brain barrier and reach brain parenchyma in a concentration sufficient to elicit neuroprotection, as suggested by i) its polyphenol-like structure compatible with a potent free radical scavenging activity, ii) its capability to complex iron rendering it inactive to catalyze reactive oxygen species formation, and iii) its high QPlogP octanol/water of 6.449 (theoretical value).

Several free radical scavenging drugs are present in vivo at concentrations that would allow them to compete with biological molecules for reaction with $^{\bullet}OH$ or HOCl; in order to compete, a scavenger must to be present at no less than millimolar concentrations (45). Thus, it is possible that GA never achieves this concentration range. However, an antioxidant strategy in the human body is the safe sequestration of iron or copper ions into forms that do not catalyze this free radical formation. In this regard, we believe that GA, in a concentration perfectly reachable in vivo, protects neuronal cells from damage induced by iron mainly through its iron-complexing capability.

Other mechanisms reported for protection of neuronal cells from oxidative damage are the following: i) direct free radical/reactive oxygen species scavenging capability and ii) inhibition of stress-induced caspases activation (46). In fact, garcinol, a prenylated benzophenone structurally related with GA, presents potent free radical scavenging activity (47) and enhances neuronal survival in neuron-astrocyte co-cultures with lipopolysaccharide (LPS) treatment, reducing the expression of LPS-induced inflammatory mediators (48).

Our present results show for the fist time a potential of GA against neuronal diseases associated with iron-induced oxidative stress, as long as iron has been implicated in the neuropathology of several neurodegenerative disorders (2 – 6) and cerebral ischemia (49, 50).

Acknowledgments

This work was partially supported by CAPES-Brazil/MES-Cuba (064/09) and by International Foundation of Science (IFS) grants F/4450-1 and IFS 4905. The excellent technical assistance of Dr. Lázara Castillo is also gratefully acknowledged.

References

1 Youdim MB, Fridkin M, Zheng H. Bifunctional drug derivatives of MAO-B inhibitor rasagiline and iron chelator VK-28 as a more effective approach to treatment of brain ageing and ageing neurodegenerative diseases. Mech Ageing Dev. 2005;126:317–326.

2 Bolognin S, Messori L, Zatta P. Metal ion physiopathology in neurodegenerative disorders. Neuromolecular Med. 2009;11: 223–238.

3 Berg D. In vivo detection of iron and neuromelanin by transcranial sonography – a new approach for early detection of substantia nigra damage. J Neural Transm. 2006;113:775–780.

4 Castellani RJ, Moreira PI, Liu G, Dobson J, Perry G, Smith MA, et al. Iron: the Redox-active center of oxidative stress in Alzheimer disease. Neurochem Res. 2007;32:1640–1645.

5 Double KL, Gerlach M, Youdim MB, Riederer P. Impaired iron homeostasis in Parkinson's disease. J Neural Transm. 2000;60: 37–58.

6 Halliwell B. Oxidative stress and neurodegeneration: where are we now. J Neurochem. 2006;97:1634–1658.

7 Meissner W, Hill MP, Tison F, Gross CE, Bezard E. Neuroprotective strategies for Parkinson's disease: conceptual limits of animal models and clinical trials. Trends Pharmacol Sci. 2004;25:249–253.

8 Jiang H, Luan Z, Wang J, Xie J. Neuroprotective effects of iron chelator Desferal on dopaminergic neurons in the substantia nigra of rats with iron-overload. Neurochem Int. 2006;49:605–609.

9 Carbonell T, Rama R. Iron, oxidative stress and early neurological deterioration in ischemic stroke. Curr Med Chem. 2007;14: 857–874.

10 Zheng H, Weiner LM, Bar-Am O, Epsztejn S, Cabantchik ZI, Warshawsky A, et al. Design, synthesis, and evaluation of novel bifunctional iron-chelators as potential agents for neuroprotection in Alzheimer's, Parkinson's, and other neurodegenerative diseases. Bioorg Med Chem. 2005;13:773–783.

11 Kupershmidt L, Weinreb O, Amit T, Mandel S, Carri MT, Youdim MB. Neuroprotective and neuritogenic activities of novel multimodal iron-chelating drugs in motor-neuron-like NSC-34 cells and transgenic mouse model of amyotrophic lateral sclerosis. FASEB J. 2009;23:3766–3779.

12 Hanson LR, Roeytenberg A, Martinez PM, Coppes VG, Sweet DC, Rao RJ, et al. Intranasal deferoxamine provides increased brain exposure and significant protection in rat ischemic stroke. J Pharmacol Exp Ther. 2009;330:679–686.

13 Youdim MB, Stephenson G, Ben Shachar D. Ironing iron out in Parkinson's disease and other neurodegenerative diseases with iron chelators: a lesson from 6-hydroxydopamine and iron chelators, desferal and VK-28. Ann N Y Acad Sci. 2004;12:306–325.

14 Zheng H, Blat D, Fridkin M. Novel neuroprotective neurotrophic NAP analogs targeting metal toxicity and oxidative stress: potential candidates for the control of neurodegenerative diseases. J Neural Transm Suppl. 2006;71:163–172.

15 Guo Q, Zhao B, Li M, Shen S, Xin W. Studies on protective mechanisms of four components of green tea polyphenols against lipid peroxidation in synaptosomes. Biochim Biophys Acta. 1996;1304:210–222.

16 Ono K, Yoshiike Y, Takashima A, Hasegawa K, Naiki H, Yamada M. Potent anti-amyloidogenic and fibrildestabilizing effects of polyphenols in vitro: implications for the prevention and therapeutics of Alzheimer's disease. J Neurochem. 2003;87:172–181.

17 Levites Y, Amit T, Mandel S, Youdim MBH. Neuroprotection and neurorescue against Aβ toxicity and PKC dependent release of nonamyloidogenic soluble precursor protein by green tea polyphenol (-)-epigallocatechin-3-gallate. FASEB J. 2003;17: 952–954.

18 Gustafson KR, Blunt JW, Munro MHG, Fuller RW, McKee TC, Cardellina JH, et al. The guttiferones, HIV-inhibitory benzophenones from Symphonia globulifera, Garcinia livingstonei, Garcinia ovalifolia and Clusia rosea. Tetrahedron. 1992;48:10093–10102.

19 Williams RB, Hoch J, Glass TE, Evans R, Miller JS, Wisse JH, et al. A novel cytotoxic guttiferone analogue from Garcinia macrophylla from the Suriname Rainforest. Planta Med. 2003;69: 864–866.

20 Ngouela S, Lenta BN, Noungoue DT, Ngoupayo J, Boyom FF, Tsamo E, et al. Anti-plasmodial and antioxidant activities of constituents of the seed shells of Symphonia globulifera Linn f. Phytochemistry. 2006;67:302–306.

21 Pereira IO, Marques MJ, Pavan ALR, Codonho BS, Barbieri CL,

Beijo LA, et al. Leishmanicidal activity of benzophenone sand extracts from *Garcinia brasiliensis* Mart. Fruits. Phytomedicine. 2010;17:339–345.

22 Cuesta-Rubio O, Padrón A, Velez Castro H, Pizza C, Rastrelli L. Aristophenones A and B. A new tautomeric pair of polyisoprenylated benzophenones from *Garcinia Aristata*. J Nat Prod. 2001; 64:973–975.

23 Whittemore ER, Loo DT, Watt JA, Cotman CW. A detailed analysis of hydrogen peroxide-induced cell death in primary neuronal culture. Neuroscience. 1995;67:921–932.

24 Hermes-Lima M, Castilho RF, Meinicke AR, Vercesi AE. Characteristics of Fe(II) ATP complex-induced damage to the rat liver mitochondria. Mol Cell Biochem. 1995;145:53–60.

25 Genet S, Kale RK, Baquer NZ. Alterations in antioxidant enzymes and oxidative damage in experimental diabetic rat tissues: effect of vanadate and fenugreek (Trigonellafoenum graecum). Mol Cell Biochem. 2002;236:7–12.

26 Buege JA, Aust SD. Microsomal lipid peroxidation. Methods Enzymol. 1978;52:302–310.

27 Aruoma OI. Deoxyribose assay for detecting hydroxyl radicals. Methods Enzymol. 1994;23:57–66.

28 Pariente F, Lorenzo E, Abruna HD. Electrocatalysis of NADH oxidation with electropolymerized films of 3,4-dihydroxybenzaldehyde. Anal Chem. 1994;66:4337–4344.

29 Qu W, Fan L, Kim YC, Ishikawa S, Iguchi-Ariga SM, Pu XP, et al. Kaempferol derivatives prevent oxidative stress–induced cell death in a DJ-1–dependent manner. J Pharmacol Sci. 2009; 110:191–200.

30 Nishida H, Kushida M, Nakajima Y, Ogawa Y, Tatewaki N, Sato S, et al. Amyloid-β-induced cytotoxicity of PC-12 cell was attenuated by *Shengmai-san* through redox regulation and outgrowth induction. J Pharmacol Sci. 2007;104:73–81.

31 Ito Y, Shimazawa M, Akao Y, Nakajima Y, Seki N, Nozawa Y, et al. Lig-8, a bioactive lignophenol derivative from bamboo lignin, protects against neuronal damage in vitro and in vivo. J Pharmacol Sci. 2006;102:196–204.

32 Miura H, Takano K, Kitao Y, Hibino S, Choshi T, Murakami R, et al. A carbazole derivative protects cells against endoplasmic reticulum (ER) stress and glutathione depletion. J Pharmacol Sci. 2008;108:164–171.

33 Cho SO, Ban JY, Kim JY, Jeong HY, Lee IS, Song KS, et al. *Aralia cordata* protects against amyloid β protein (25-35)–induced neurotoxicity in cultured neurons and has antidementia activities in mice. J Pharmacol Sci. 2009;111:22–32.

34 Cheng HY, Hsieh MT, Wu CR, Tsai FH, Lu TC, Hsieh CC, et al. Schizandrin protects primary cultures of rat cortical cells from glutamate-induced excitotoxicity. J Pharmacol Sci. 2008;107: 21–31.

35 Hiroi M, Ogihara T, Hirano K, Hasegawa M, Morinobu T, Tamai H, et al. Regulation of apoptosis by glutathione redox state in PC12 cells exposed simultaneously to iron and ascorbic acid. Free Radic Biol Med. 2005;38:1057–1072.

36 Pardo-Andreu G, Sánchez-Baldoquín C, Ávila-González R, Delgado R, Naal Z, Curti C. Fe(III) improves antioxidant and cytoprotecting activities of mangiferin. Eur J Pharmacol. 2006; 547:31–36.

37 Pardo-Andreu GL, Sánchez-Baldoquín C, Avila-González R, Yamamoto ET, Revilla A, Uyemura SA, et al. Interaction of Vimang (Mangifera indica L. extract) with Fe(III) improves its antioxidant and cytoprotecting activity. Pharmacol Res. 2006;54: 389–395.

38 Pardo-Andreu GL, Cavalheiro RA, Dorta DJ, Naal Z, Delgado R, Vercesi AE, et al. Fe(III) shifts the mitochondria permeability transition-eliciting capacity of mangiferin to protection of organelle. J Pharmacol Exp Ther. 2007;320:646–653.

39 Welch KD, Davies TZ, Aust SD. Iron autoxidation and free radical generation: effects of buffer, ligands and chelators. Arch Biochem Biophys. 2002;397:360–369.

40 Andreu GP, Delgado R, Velho JA, Curti C, Vercesi AE. Iron complexing activity of mangiferin, a naturally occurring glucosylxanthone, inhibits mitochondrial lipid peroxidation induced by Fe^{2+}-citrate. Eur J Pharmacol. 2005;513:47–55.

41 Pardo Andreu G, Delgado R, Velho J, Inada NM, Curti C, Vercesi AE. Mangifera indica L. extract (Vimang) inhibits Fe^{2+}-citrate-induced lipoperoxidation in isolated rat liver mitochondria. Pharmacol Res. 2005;51:427–435.

42 Pardo-Andreu GL, Delgado R, Núñez-Sellés AJ, Vercesi AE. Dual mechanism of mangiferin protection against iron-induced damage to 2-deoxyribose and ascorbate oxidation Pharmacol Res. 2006;53:253–260.

43 Pardo-Andreu GL, Delgado R, Núñez-Sellés AJ, Vercesi AE. Mangifera indica L. extract (Vimang) inhibits 2-deoxyribose damage induced by Fe (III) plus ascorbate. Phytother Res. 2006;20:120–124.

44 Halliwell B, Gutteridge JMC. Antioxidant defenses. In: Halliwell B, Gutteridge JMC, editors. Free radical in biology and medicine, 3rd ed. Oxford: Oxford University Press; 1999. p. 105–245.

45 Halliwell B. Drug antioxidant effects. A basis for drug selection? Drugs. 1991;42:569–605.

46 Martins FT, Assis DM, Dos Santos MH, Camps I, Veloso MP, Juliano MA, et al. Natural polyprenylated benzophenones inhibiting cysteine and serine proteases. Eur J Med Chem. 2009;44: 1230–1239.

47 Yamaguchi F, Saito M, Ariga T, Yoshimura Y, Nakazawa H. Free radical scavenging activity and antiulcer activity of Garcinol from Garcinia indica fruit rind. J Agric Food Chem. 2000;48: 2320–2325.

48 Lia C-H, Ho C-T, Lin J-K. Effects of garcinol on free radical generation and NO production in embryonic rat cortical neurons and astrocytes. Biochem Biophys Res Comm. 2005;329:1306–1314.

49 Millan M, Sobrino T, Castellanos M, Nombela F, Arenillas JF, Riva E, et al. Increased body iron stores are associated with poor outcome after thrombolytic treatment in acute stroke. Stroke. 2007;38:90–95.

50 Erdemoglu AK, Ozbakir S. Serum ferritin levels and early prognosis of stroke. Eur J Neurol. 2002;9:633–637.